Fractured Volcanic Reservoir Characterization: A Case Study in the Deep Songliao Basin*

Desheng Sun[1], Ling Yun[1], Gao Jun[1], Xiaoyu Xi[1], and Jixiang Lin[1]

Search and Discovery Article #10584 (2014)
Posted March 30, 2014

*Adapted from extended abstract prepared in conjunction with oral presentation at AAPG 2014 Annual Convention and Exhibition, Houston, Texas, April 6-9, 2014,

[1]BGP CNPC, Zhuozhou, Hebei, China (dshsun@163.com)

Abstract

The study area is located in the XJ fault depression, within the deep Songliao basin of northeastern China. The area is characterized by a monoclinal structure that includes a few fractured volcanic reservoir traps in Cretaceous formations. The P&D of gas reservoirs faced many difficulties, including imaging of the volcano, identification of heterogeneous volcanic rock facies, and fracture detection, which was the most important. Based on the integrated acquisition and processing of 3D-VSP and full-azimuth surface seismic data, this paper focuses on the interpretation of volcanic reservoirs to characterize the fractured volcanic reservoir geometry, distribution, properties and highly productive gas regions.

Use of seismic attributes for fractured volcanic reservoirs' detection below the resolution of conventional seismic data is a major goal in this project. A new method is developed to improve imaging of volcanoes, and minor faults and fractures using "discrete frequency curvature (DFC)". The DFC data are computed using discrete frequency seismic data obtained from spectral decomposition. The DFC attribute allows us to recognize different geologic information about fractured volcanic reservoirs in different frequency bands of seismic data. The low-frequency curvature data can be used to recognize the distribution of volcanoes, whereas high-frequency curvature data is more effective at detecting minor faults and fractures. Moreover, the multi-geophysical methods, such as strata slice, HTI fracture detection and pre-stack inversion etc., also have been applied to characterize the volcanic reservoir. Strata time slices of coherence data are used to describe the volcanic evolution. Structure modelling can provide an efficient tool to delineate geometry and distribution of volcanic bodies. The fracture inversion and HTI fracture detection method can be used to detect the orientation and density of fractured reservoir, while AVO and pre-stack inversion is applied to detect gas-bearing volcanic reservoirs.

After integrated study of the seismic attributes, well logs, and production data, we predicted the favourable production zones within the volcanic reservoir. The main factors controlling the volcanic reservoir are the distribution of volcanic facies, small faults, and fractures. The hydrocarbon reservoirs are located at a high position within the volcanoes, and the hydrocarbon is clustered around the small faults and fractures within the system.

Introduction

The study area is located in the XJ fault depression within the deep Songliao basin of northeastern China, where there is a large amount of natural gas in the Mesozoic volcanic rock traps. The formation and distribution of volcanic gas reservoirs in the XJ fault depression is mainly controlled by the basement fracture system, volcanic rock facies, palaeohigh, the source rock distributed area and the volcanic cap rock.

Natural fractures and faults in the volcanic reservoirs have an important role in fluid flow and accumulation. The effective reservoir spaces of the volcanic reservoirs are the pore spaces and fractures. Fractures can not only act as reservoir spaces, but can also interconnect the pore spaces between different types of rocks and promote dissolution at later stages (Liu, 2004). The types of reservoir spaces in volcanic reservoirs are also controlled by the facies. The volcanic reservoirs found in various facies belts have quite different pore spaces, fractures, and their assemblages (Wang et al. 2003).

Use of seismic attributes for fractured volcanic reservoirs detection below the resolution of conventional seismic data is a major goal in the study of this project. Since the development of the coherence cube (Bahorich and Farmer, 1995), seismic attributes have played an important role in detecting faults and fractures in the earth's crust. Other coherence algorithms (e.g. Marfurt et al., 1998; Gersztenkorn and Marfurt, 1999) have been applied to improve the quality of images of faults and fractures. Curvature attributes (Roberts, 2001) are widely now used to enhance the resolution of faults and fractures. However, all these investigations are based on full- or dominant-spectrum seismic data. Spectral decomposition (Partyka et al., 1999) provides a novel means of utilizing seismic data, and a method called "time-frequency 4-D cube" was developed to extract seismic information from seismic data based on the different geologic scales in different frequency bands. Using these methods, discrete frequency coherence cubes (Sun et al., 2010) can be applied to detect faults and fracture zones that cannot be easily detected using the full spectrum coherence data.

By integrating the advantages of curvature and spectral decomposition, we developed another method to improve the imaging of faults and fractures called "discrete frequency curvature (DFC)," that permits the detection of fractured volcanic reservoirs. This method is computed using discrete frequency seismic data obtained from spectral decomposition. The results of our case study show that this has the potential to be a valuable and highly effective seismic method.

Moreover, the multi-geophysical methods also applied on the interpretation of volcanic reservoirs to characterize the volcanic reservoir geometry, distribution, internal structure, reservoir properties and high gas production regions.

Background

The field area is a monoclinal structure that forms a couple of volcanic traps for the reservoirs, with depths between 3,350-3,850 meters. Five wells have been drilled in the area, but only one well had commercial gas.

Two volcanic sequences were recognized in the Mesozoic rocks of the Songliao basin, the Huoshiling sequence (J3h) and the Yincheng sequence (K1yc). Volcanic rock facies can be subdivided into marginal, transitional and central subfacies. The central subfacies, located near

the volcanic conduit, have well developed structural and contraction fractures and relatively good poroperm characteristics. As a result, it would be the most favourable reservoir facies belt. The transitional subfacies, having relatively well-developed fractures and moderate poroperm characteristics, would be a favourable reservoir facies belt. However, the marginal subfacies have poor poroperm characteristics and would be an unfavourable reservoir facies belt (Figure 1).

Because of the geologic complexities of the volcanic reservoirs in the study area, the P&D of gas reservoirs faced many difficulties, including imaging of the volcano, identification of heterogeneous volcanic rock facies, and fracture detection, which was the most important.

Seismic Data

In order to solve the above problems, a simultaneous acquisition with a 160-level large array 3D-VSP and full azimuth 3D surface seismic was employed in the AOI.

VSP-driven seismic data processing. In integrated processing of 3D-VSP and full azimuth 3D surface seismic data, we employed a VSP-driven and reservoir focused pre-stack seismic processing flow. The processing flow includes: time-frequency domain spherical spreading and absorption compensation (Gao et al. 2004) for the near-surface and earth absorption effects, two-step statistical deconvolution of both shot and receiver gathers (Ling et al. 1998) aimed at suppression of land reverberation and removal of the spatial wavelet difference. A geophysical QC procedure (Gao et al. 2009) is implemented in all major processing steps

Curvature data: After carrying out the above analysis of the volcanic reservoir in the study area, the curvature attribute was calculated and extracted from the relevant horizon in the 3-D seismic data (Figure 2). The results show that the curvature attribute is closely related to the fractures and volcano distribution, where the dark stripes are representative of the fault and “ring fault” systems that are representative of the volcanoes.

In the original curvature map, there are three volcanoes (blue arrows in Figure 2) that can be easily recognized, but the volcano (red arrow) in which well xs21-2 was drilled is difficult to interpret. The well data show that all five wells encountered well-developed factures, including isolated factures and facture clusters. With the exception of well xs21, the only well had commercial gas, the curvature attribute of the volcanic reservoir also detected minor faults at the location of the remaining wells. In an effort to understand these relations, we used the discrete frequency curvature data.

Discrete Frequency Curvature

Faults and fractures occur on many scales in the Earth. Therefore, we can detect faults and fractures found at different scales using different frequency bands. Discrete frequency curvature is a method that uses curvature data and the discrete Fourier transform (DFT) to detect fractured reservoirs. Theoretical analysis shows that at different scales, geologic information can be detected in different frequency bands of seismic data, where the high frequency component is more sensitive to subtle perturbations in the seismic character. This method allows detection of subtle

faults, fractures, and other geologic information that are not easily observed through dominant-spectrum seismic data. This analysis is performed in the following three steps:

1) Computation is done via running spectral analysis, which calculates the amplitude spectrum of the input seismic volume. From the input seismic volume, discrete frequency seismic cubes are computed into multiple discrete frequency volumes by digital filtering in the effective frequency band. The spectral components are then sorted into common frequency component cubes.
2) The discrete frequency curvature data are calculated with the same curvature algorithm and processing parameter using the discrete frequency data previously calculated via spectral decomposition.
3) After interpreting the multi-scale frequency curvature data, favourable discrete curvature data that reveal geologic information about the fractured reservoir are selected for volume merging and reconstruction to create a new set of curvature data.

Spectral analysis shows that the bandwidth of seismic data of the study area is about 10-55 Hz. Therefore, 10 discrete frequency bands are calculated by increasing frequency sampling by 5 Hz.

Figure 3 shows the four maps of the volcanic reservoir (at 20 Hz, 30 Hz, 40 Hz and 50 Hz) determined from the 10 discrete frequency curvature data. These data yield better spatial resolution for imaging volcanoes and faults, and can be used to determine the spatial extent of extensive fracturing. Figure 3a shows a discrete frequency curvature map of 20 Hz of the volcanic reservoir. In this map, some volcanoes (red arrows), including the xs21-2 volcano, are more clear than that in the original curvature map. In Figure 3b, we can see a close relationship between the 30 Hz band and the original curvature maps because the main frequency is about 30 Hz, but Figure 3b shows more details of the fault and fracture distribution. For example, at the location of the red arrow, some minor faults (or fracture zones) can be interpreted that are not easily seen in the original curvature. In Figure 3c and 3d, the higher frequency curvature data gives greater detail of the minor faults and fractures. In the 50 Hz curvature map, small faults or fractures can finally be detected at the location of well xs21.

After the interpretation of the multi-scale frequency data, favourable discrete frequency curvature data that reveal volcanoes, and faults and fracture distribution were selected to create a new curvature cube by means of volume merging and reconstruction. Figure 4 shows a reconstructed curvature map (20 Hz and 50 Hz). Compared with the original curvature map, it offers a higher level of detail for the volcanoes, faults, and fractures.

Integrated Study and Results

The multi-geophysical methods such as volcanic rock modelling and HTI fracture detection techniques are also used to characterize the volcanic reservoir geometry, distribution and reservoir properties. Structural modelling using seismic and coherence data provides an efficient tool to delineate distributions of the volcanic rock body and fault systems. The spatial change of the HTI media can be used to compute the orientation and density of fractures in the volcanic reservoir. The pre-stack inversion tool is used to detect gas-bearing volcanic reservoirs.

The evolution of the volcano: In order to study the evolution of the volcano, the strata from the basement of Huoshiling (T5) to the top of the volcanic rocks of Yincheng (T4c) was divided into 20 layers proportionally and 20 strata slices of coherence data was extracted in the time domain (Figure 5).

The deep zone fault system dominates the distribution of the volcanic massif and volcanic facies. In the T5 strata slices of the coherence data, there are two-ring incoherence zones (location of red circle) located in the basement fracture system of NW direction, which indicates the position of the volcanic crater. With increasing of time, more volcanic craters could be identified in strata slices of the coherence volume, and the distribution of volcanic craters changed to a nearly north-south direction.

The structural modelling of the central volcanic subfacies: The volcanic reservoir geometry can be built with structural modelling. Based on the interpretation of seismic data of the strata slice of coherence data, we obtain a group of point set of the central volcanic subfacies which has well developed structural and contraction fractures and create a structural model using the proper interpolation formula (Figure 6). The volcanic rocks are characterized by high-level eruption and low-level filling, and have a greater thickness along the crater.

Computation of the fracture orientation and density: Relative spatial changes of the HTI media are directly related to the fracture pattern in the AOI (Sun et al. 2009). With the earlier study results and the latest research, the fracture orientation and density can be calculated along a horizon by the azimuthal gather of the full-azimuth seismic data (Figure 7). The result shows that the fracture is closely related to the coherence attributes as well as the fracture density map obtained from the fracture inversion. In Figure 7a, the arrows show the position of the ring faults overlaid by the “ring fracture system” which have higher fracture density (Figure 7b).

Most of the fracture zone, which is controlled by volcanic activity distributed around the central volcanic subfacies, has relatively good poroperm characteristics and it would be the most favourable volcanic reservoir belt in the AOI.

The detection of gas-bearing volcanic reservoirs: Based on the inversion of pre-stack seismic data, Poisson’s ratio was calculated. As shown in Figure 8a, the high gas production well (xs21) is located in a region where the Poisson’s ratio is high, and the other four dry or low gas production wells are located in regions with low Poisson’s ratios. This indicates a high correlation between the gas production and Poisson’s ratio. Figure 8b is an integrated display which overlays the Poisson’s ratio on a 3D time structure map, all of the high Poisson’s ratio regions have good volcanic structure backgrounds which formed traps for the accumulation of natural gas.

Result: After integrated study of the multi-geophysical methods, well logs, and production data, we predicted the favourable production zones within the volcanic reservoir. The main factors controlling the volcanic reservoir are the distribution of volcanoes, small faults, and fractures. The hydrocarbon reservoirs are located at a high position within the volcanoes, and the hydrocarbon is clustered around the small faults and fractures within the system. Based on the results of this study, a very productive well was drilled in a region that was predicted to be enriched in hydrocarbons (Figure 9).

Conclusions

After interpretation of the VSP-driven processed full-azimuth seismic data, the following conclusions can be made:

1. The discrete frequency curvature attributes reflect more geologic information of volcanic reservoirs than full spectrum data. The different discrete frequency curvature attribute maps show that low-frequency data can be used to recognize the distribution of volcanoes, and high-frequency data can more effectively detect faults and fractures. Therefore, the reconstructed curvature data offers a greater level of detail for the fractured volcanic reservoir than the full spectrum data.

2. Research results show that modelling of volcanic rocks integrated with the fracture detection can guide the predictions of volcanic reservoir distributions. The reservoir properties are controlled by the volcanic rocks facies and structural characteristics.

3. The integrated study of the multi-geophysical methods, well logs, and production data is an effective way for detecting gas-bearing volcanic reservoirs.

Acknowledgements

The authors thank the Daqing Oil Company for the permission to publish the results of this study. We would also like to thank Guo Xiangyu and Sun Xiang-e for their help during implementation of this project.

References Cited

Bahorich, M.S., and S.L. Farmer, 1995, 3-D seismic discontinuity for faults and stratigraphic features: The coherence cube: SEG Expanded Abstract, p. 93-96.

Gao, J., Y. Ling, and R.J. Zhang, 2004, Spherical divergence and absorption compensation in time and frequency domain, 66th EAGE Conference & Exhibition, Extended Abstracts, P006.

Gao, J., Y. Ling, D.S. Sun, and J.X. Lin, 2009, Geophysical and geological QC in seismic data processing: SEG Expanded Abstracts, p. 624-628.

Gersztenkorn, A., and K.J. Marfurt, 1999, Eigenstructure-based coherence computations: Geophysics, v. 64, p. 1468–1479.

Ling, Y., J. Gao, and R.J. Zhang, 1998, Sand dune reverberation and its suppression: The Leading Edge, v. 17, p. 697.

Liu, W.F., 2004, Reservoir characteristics of deep volcanic rocks and prediction of favorable areas in Xujiaweizi fault depression in Songliao basin: Oil & Gas Geology, v. 25/1, p. 115-119.

Marfurt, K.J., R.L. Kirlin, S.L. Farmer, and M.S. Bahorich, 1998, 3-D seismic attributes using a semblance-based coherency algorithm: Geophysics, v. 63, p. 1150–1165.

Partyka, G., J. Gridley, and J. Lopez, 1999, Interpretational applications of spectral decomposition in reservoir characterization: The Leading Edge, v. 18/3, p. 353–360.

Roberts, A., 2001, Curvature attributes and their application to 3D interpreted horizons: First Break, v. 19, p. 85-99.

Sun, D.S., Y. Ling, X.Y. Guo, J. Gao, and J.X. Lin, 2010, Application of discrete frequency coherence cubes in the fracture detection of volcanic rocks in full-azimuth seismic data: SEG Expanded Abstracts, p. 1342-1345.

Sun, X.E., Y. Ling, J. Gao, D.S. Sun, and J.X. Lin, 2009, Anisotropic parameter estimation based on 3D VSP and full azimuth seismic data, SEG Expanded Abstract, p. 4106-4109.

Wang, P.J., S.M. Chen, W.Z. Liu, X.L. Shan, R.H. Cheng, Y. Zhang, H.B. Wu, and J.S. Qi, 2003, Relationship Between Volcanic facies and Volcanic Reservoirs in Songliao basin: Oil & Gas Geology, v. 24/1, p. 18-23.

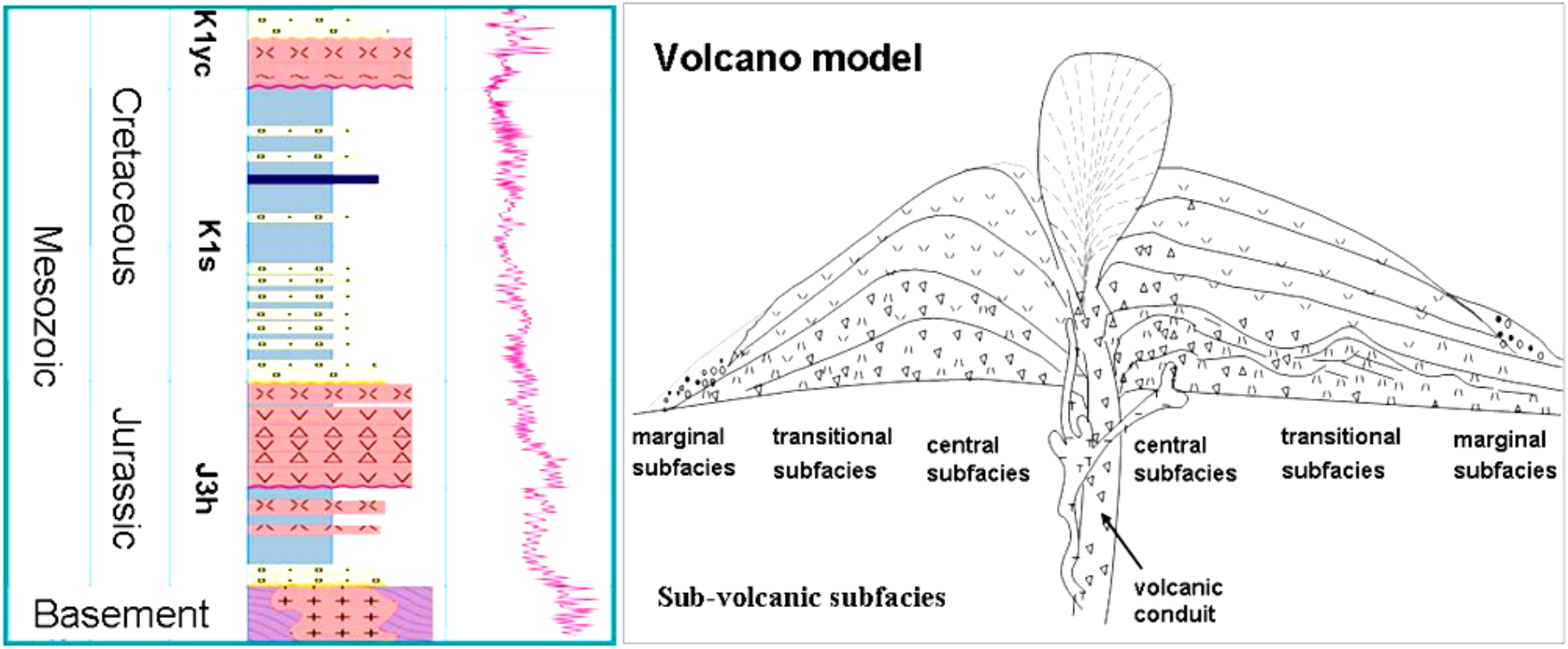

Figure 1. Left: the Mesozoic aged strata column of the Songliao basin; right: sub-volcanic subfacies of a deep zone in the XJ fault depression.

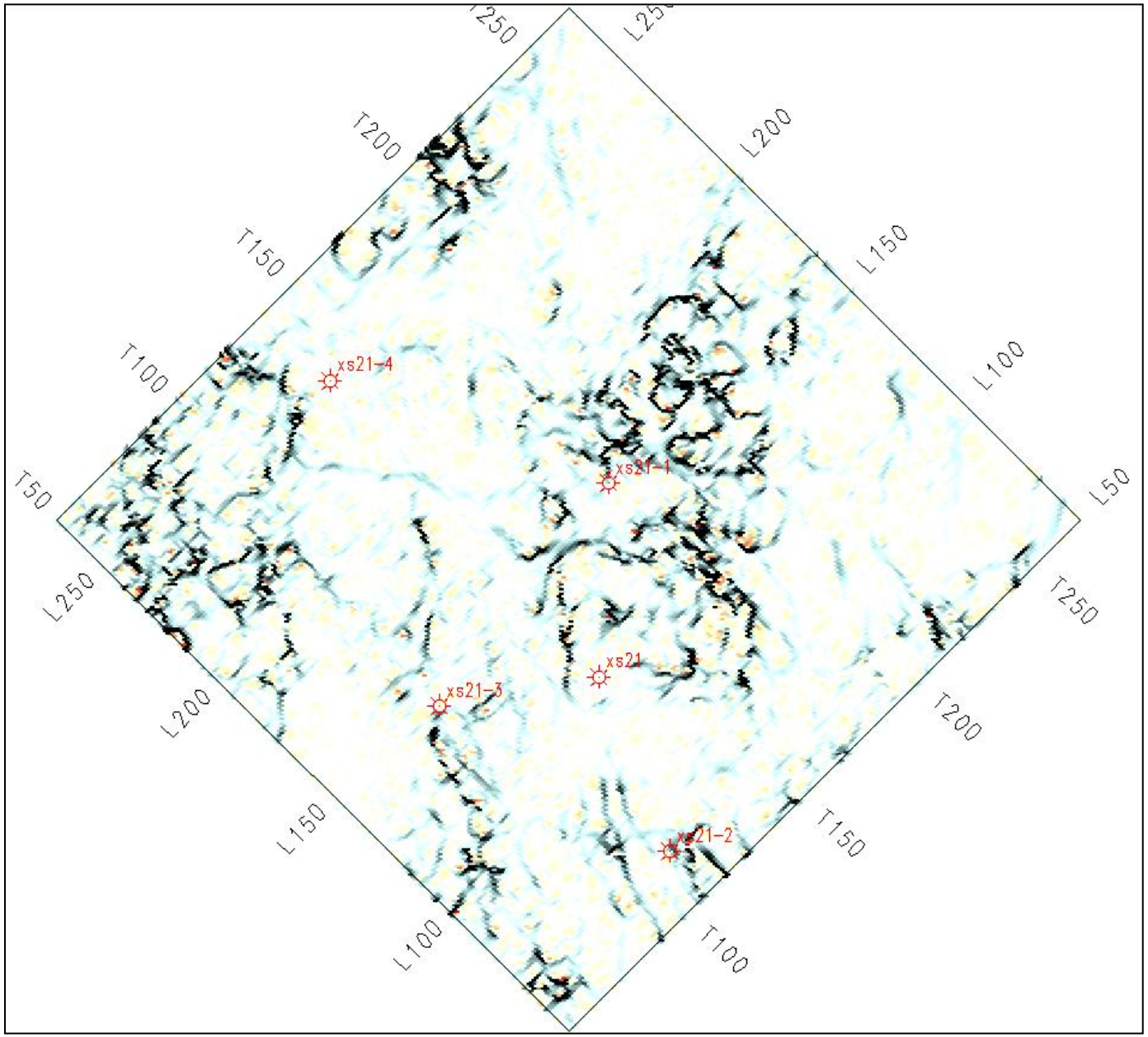

Figure 2. Curvature attribute map and well data showing detected volcanoes and fractures.

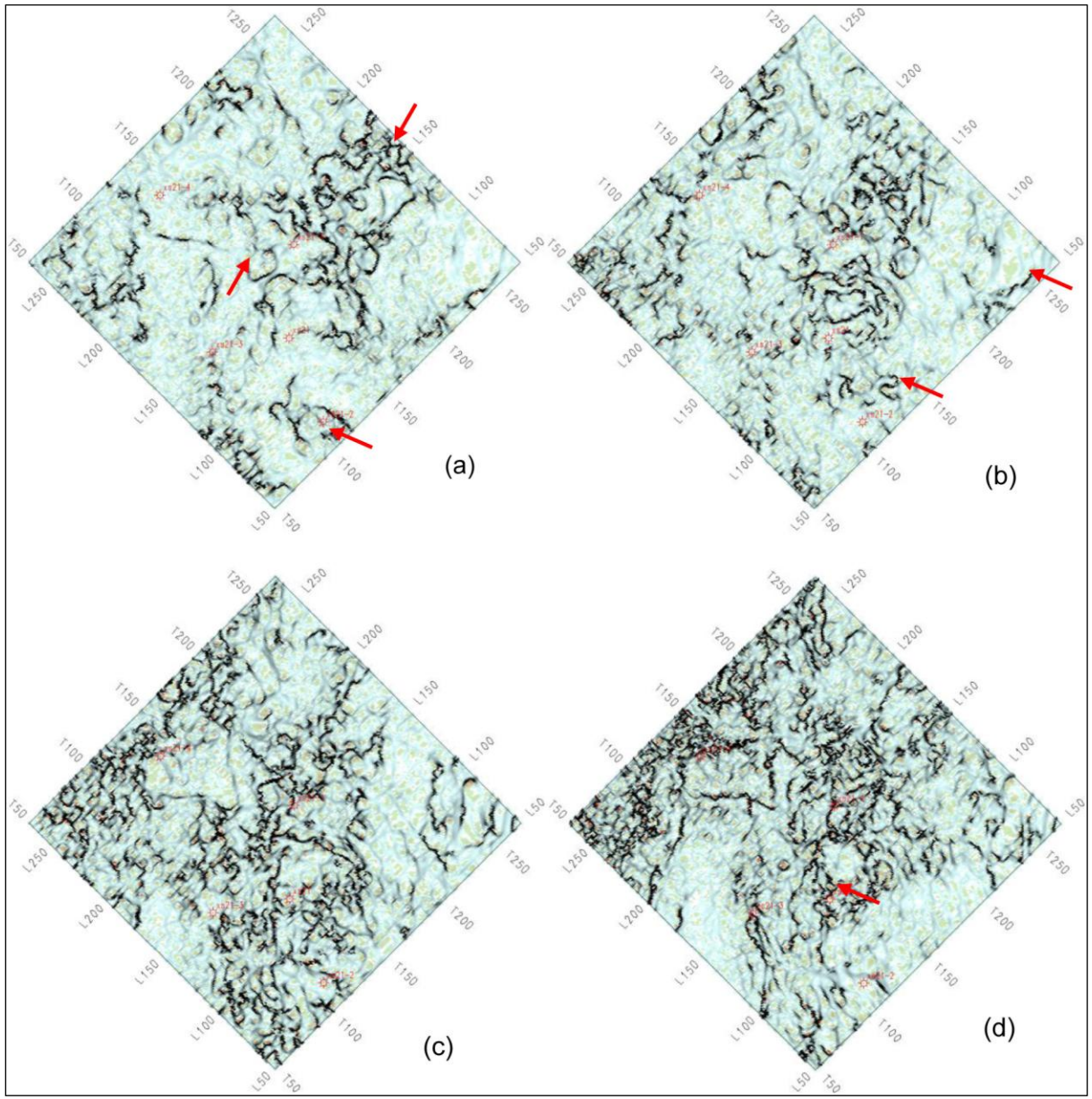

Figure 3. The discrete frequency curvature attribute maps of the volcanic reservoir (a) 20 Hz, (b) 30 Hz, (c) 40 Hz and (d) 50 Hz.

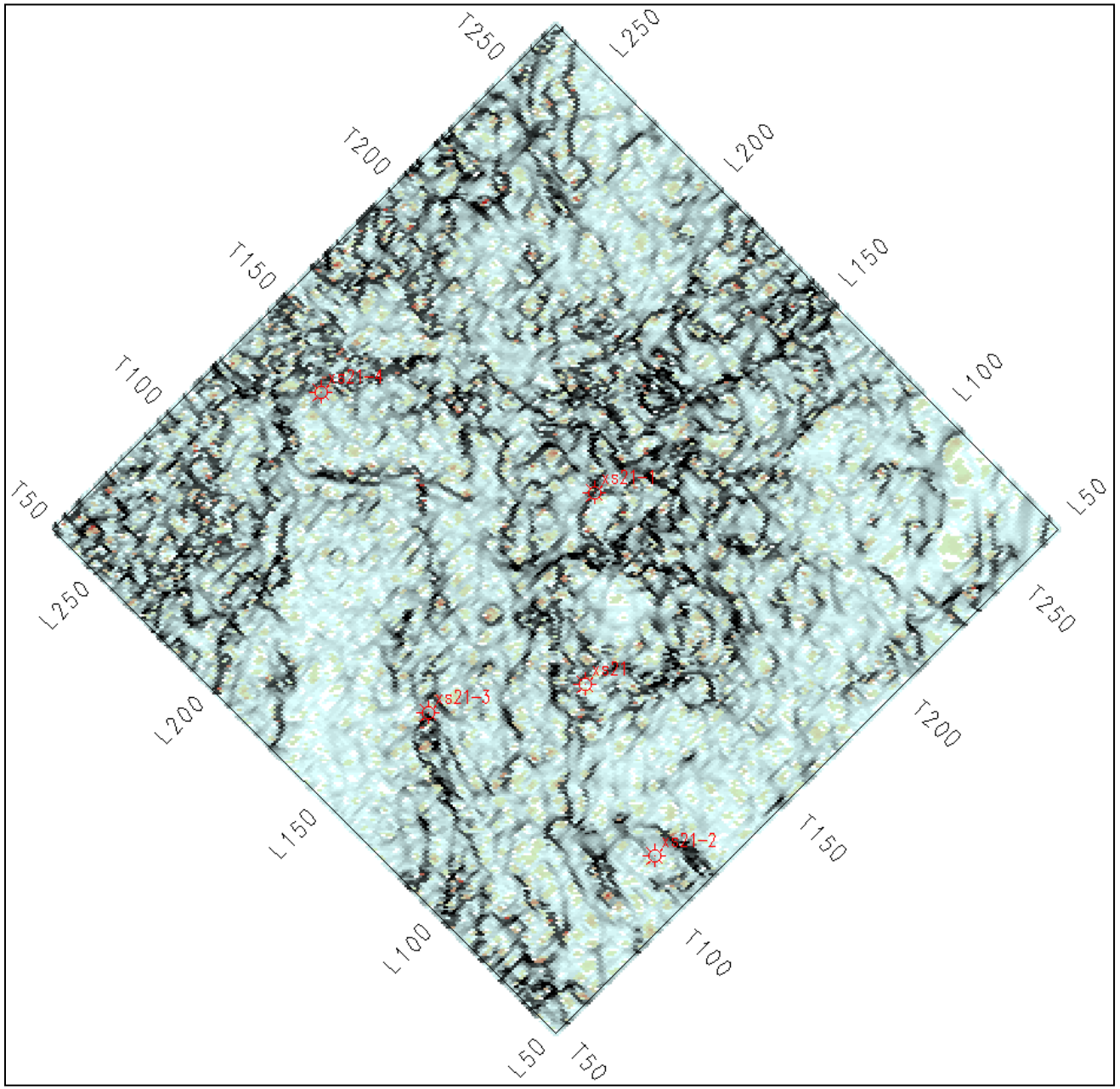

Figure 4. Reconstructed curvature attribute map of the volcanic reservoir

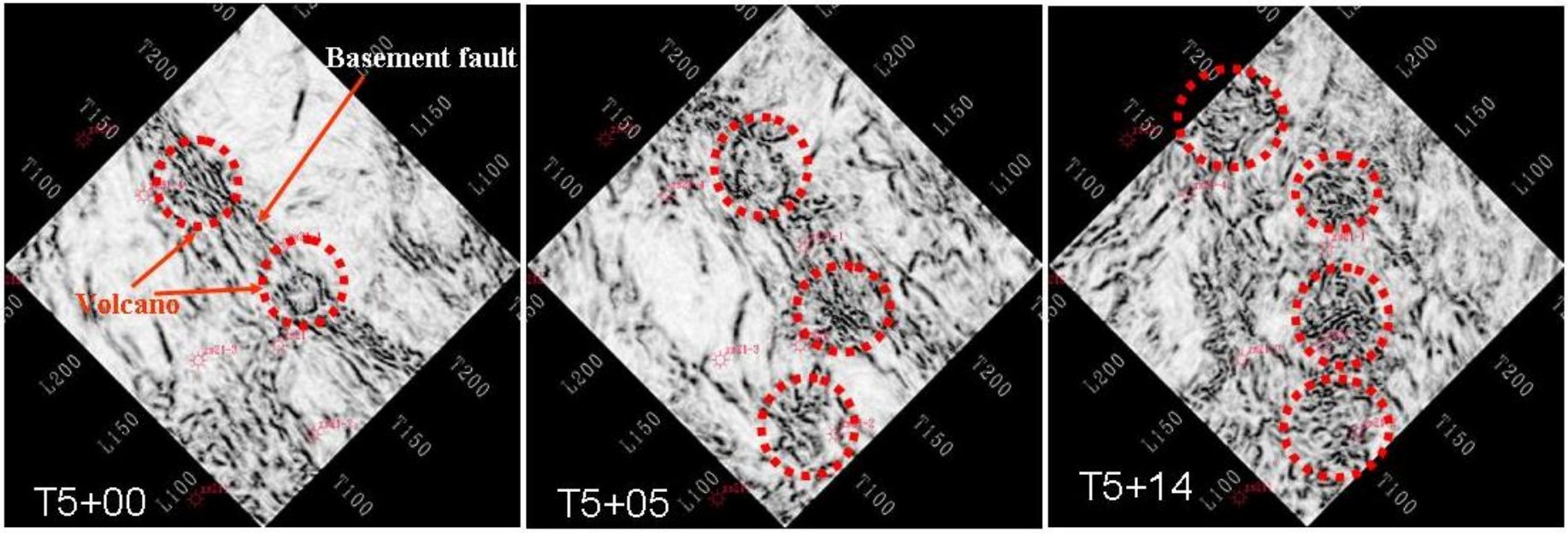

Figure 5. The spatial evolution of the volcano from the basement of Huoshiling (T5) to the top of the volcanic rocks of Yincheng (T4c).

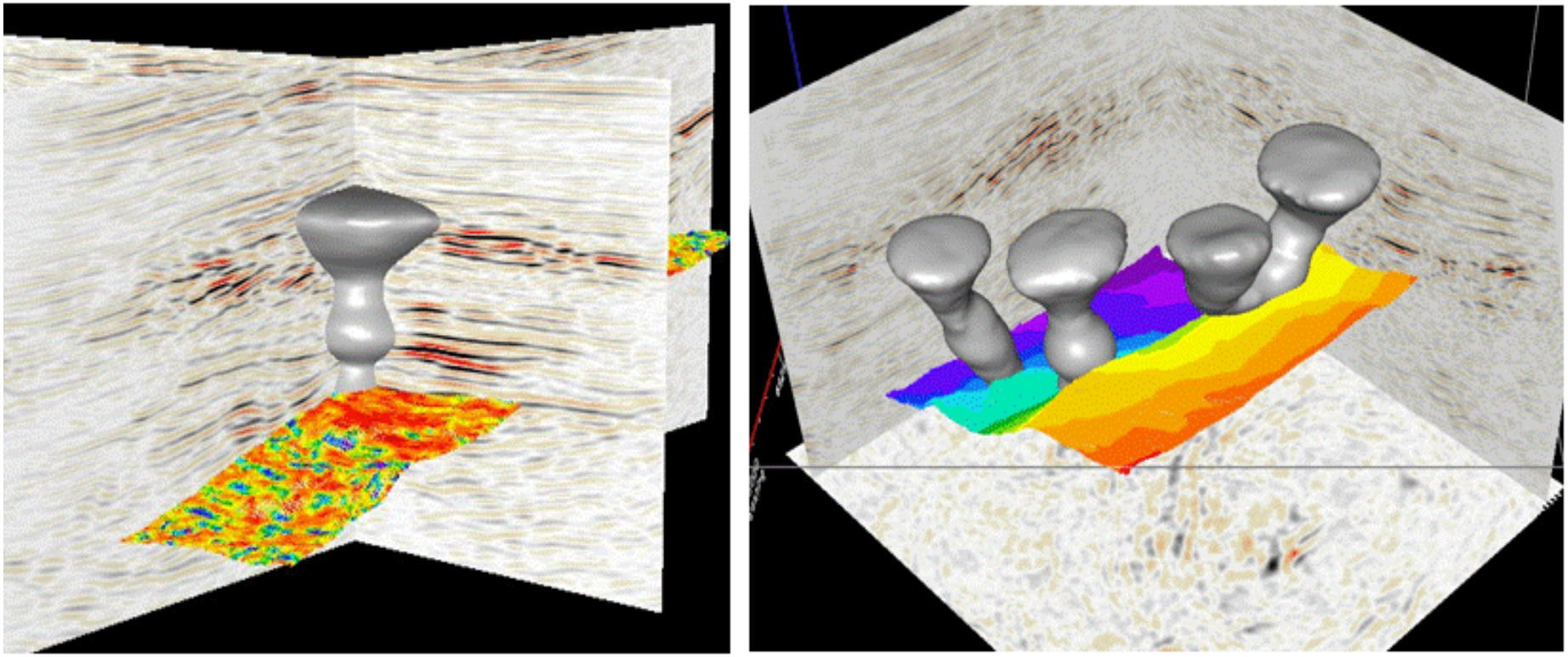

Figure 6. a) The interpretation of a volcanic rock body using strata slices of coherence and seismic data. b) The results of a volcanic rock structural modelling of the central volcanic subfacies in AOI.

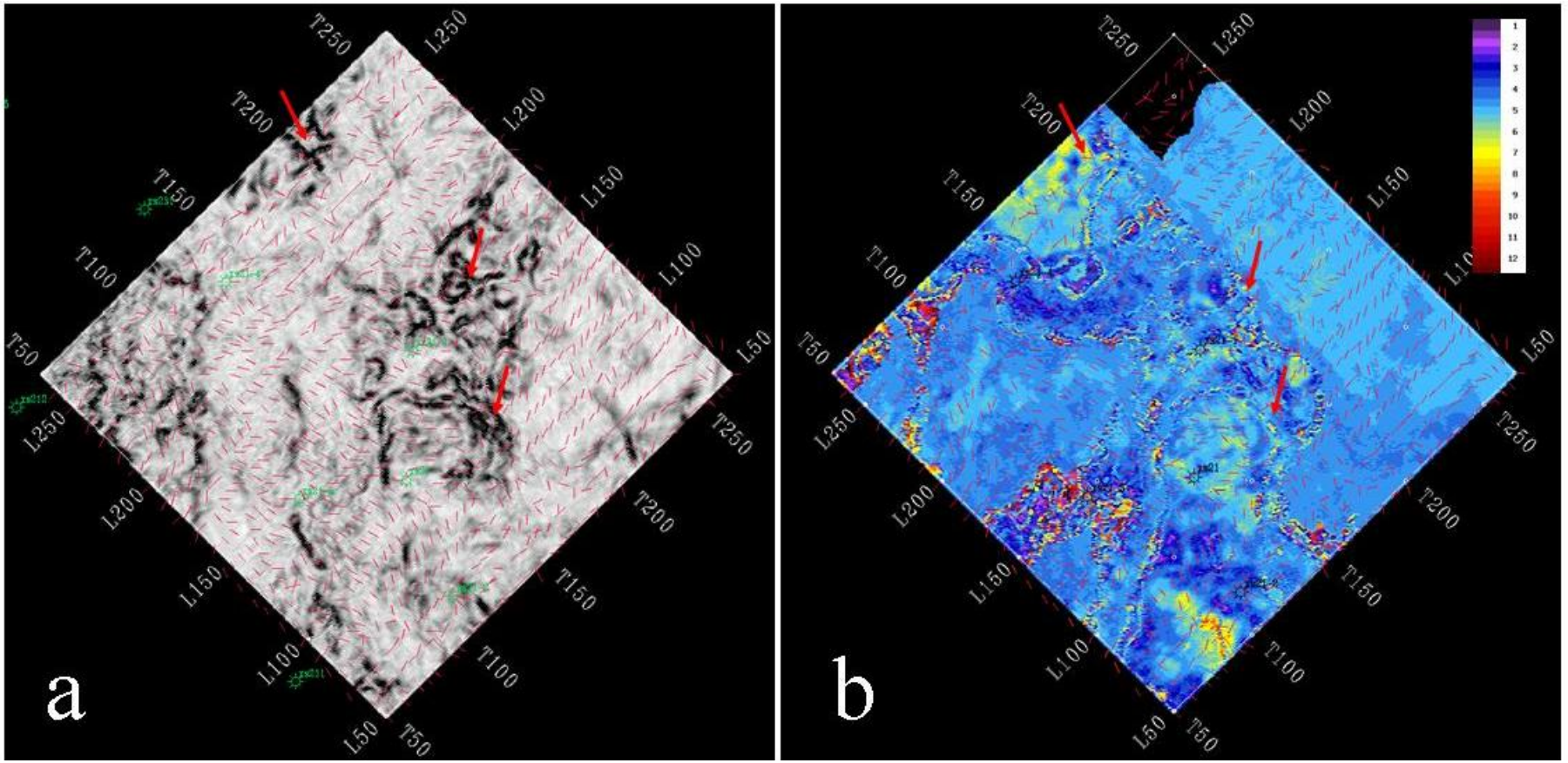

Figure 7. Fracture stick map overlaid on the coherence map (a) and fracture density map (b) on top of the volcanic rocks. The direction of the red sticks is representative of the fracture orientation and the length of the red sticks is representative of the fracture density.

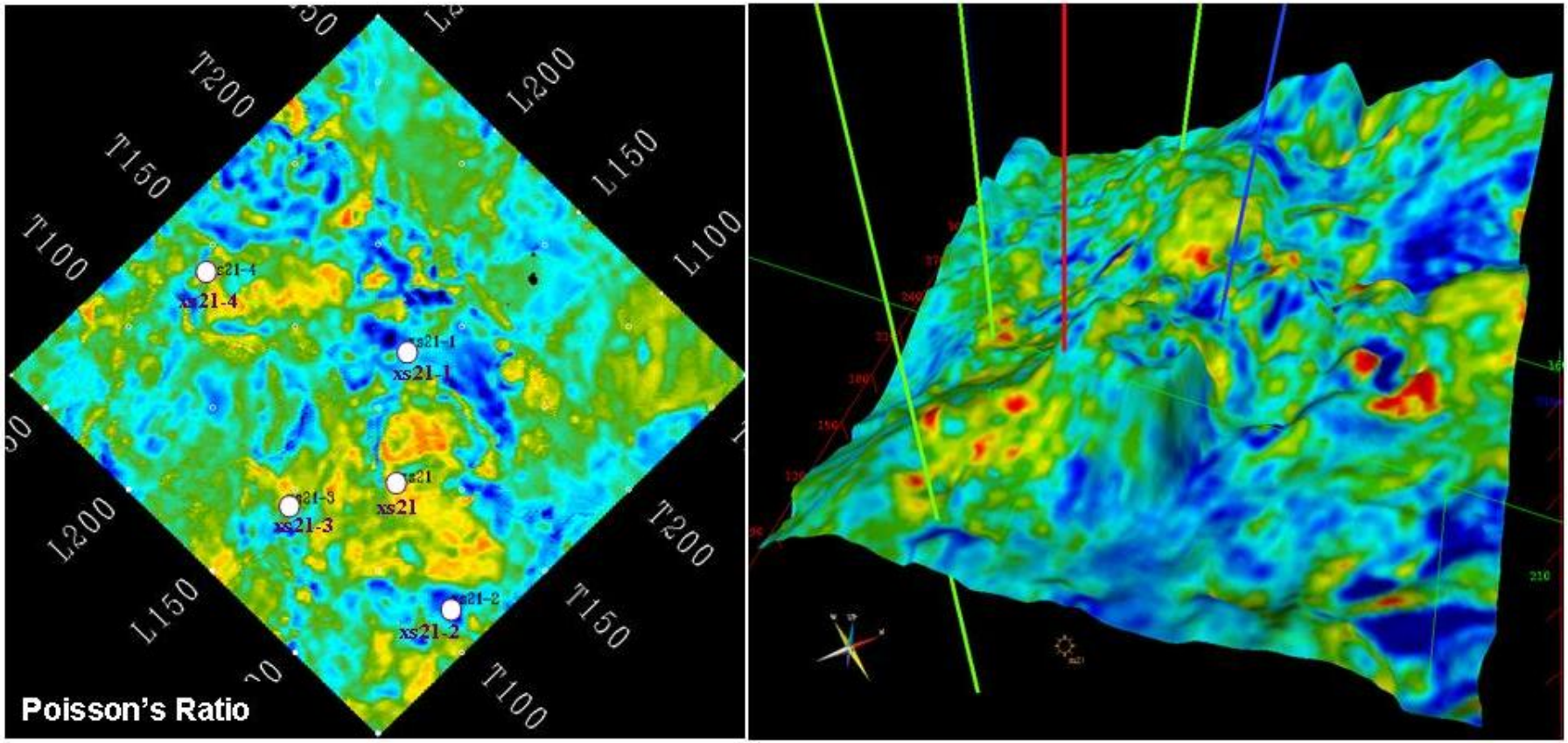

Figure 8. Poisson's ratio used to detect gas-bearing volcanic reservoirs.

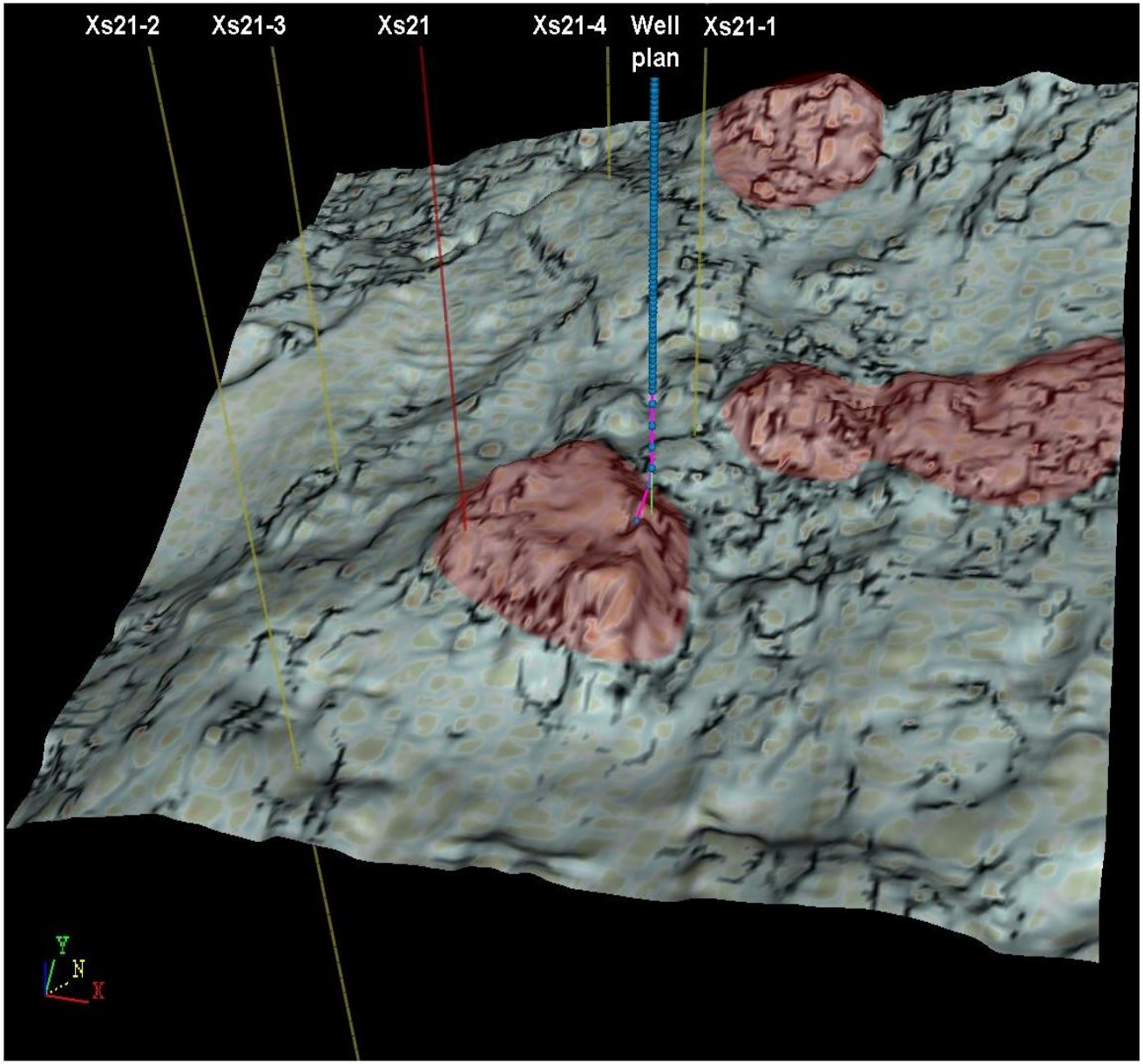

Figure 9. The prediction of hydrocarbon enriching areas in 3-D reconstructed curvature attribute map.